Visual Neuroscience (1998), **15**, 597–605. Printed in the USA.
Copyright © 1998 Cambridge University Press 0952-5238/98 $12.50

Retinal image quality in the rodent eye

PABLO ARTAL,[1] PILAR HERREROS DE TEJADA,[2] CARMEN MUÑOZ TEDÓ,[2] AND DANIEL G. GREEN[3]

[1]Laboratorio de Optica, Departamento de Física, Universidad de Murcia, Murcia, Spain
[2]Departamento de Psicobiologia, Universidad Complutense de Madrid, Madrid, Spain
[3]Department of Ophthalmology, University of Michigan, Ann Arbor

(RECEIVED July 18, 1997; ACCEPTED December 2, 1997)

Abstract

Many rodents do not see well. For a target to be resolved by a rat or a mouse, it must subtend a visual angle of a degree or more. It is commonly assumed that this poor spatial resolving capacity is due to neural rather than optical limitations, but the quality of the retinal image has not been well characterized in these animals. We have modified a double-pass apparatus, initially designed for the human eye, so it could be used with rodents to measure the modulation transfer function (MTF) of the eye's optics. That is, the double-pass retinal image of a monochromatic (λ = 632.8 nm) point source was digitized with a CCD camera. From these double-pass measurements, the single-pass MTF was computed under a variety of conditions of focus and with different pupil sizes. Even with the eye in best focus, the image quality in both rats and mice is exceedingly poor. With a 1-mm pupil, for example, the MTF in the rat had an upper limit of about 2.5 cycles/deg, rather than the 28 cycles/deg one would obtain if the eye were a diffraction-limited system. These images are about 10 times worse than the comparable retinal images in the human eye. Using our measurements of the optics and the published behavioral and electrophysiological contrast sensitivity functions (CSFs) of rats, we have calculated the CSF that the rat would have if it had perfect rather than poor optics. We find, interestingly, that diffraction-limited optics would produce only slight improvement overall. That is, in spite of retinal images which are of very low quality, the upper limit of visual resolution in rodents is neurally determined. Rats and mice seem to have eyes in which the optics and retina/brain are well matched.

Keywords: Retinal image quality, Ocular modulation transfer function, Rodent eyes

Introduction

It is well known that rodents have poor spatial vision (Lashley, 1938; Wiesenfeld & Branchek, 1976; Powers & Green, 1978; Birch & Jacobs, 1979; Balkema & Pinto, 1982; Friedman & Green, 1982; Muñoz Tedó et al., 1992; Stone & Pinto, 1993). The evidence for this comes from both electrophysiological measurements of the size of receptive fields and behavioral studies of visual acuity. Recording from single optic tract units, for example, shows that rat and mouse retinal ganglion cells have the classic center-surround receptive-field organization, but the fields are at least an order of magnitude larger than those of the primate fovea (Brown, 1965; Green et al., 1977; Balkema & Pinto, 1982; Stone & Pinto, 1993). Rat behavioral acuity under optimum conditions is only about 0.05 min^{-1} (Lashley, 1938; Wiesenfeld & Branchek, 1976; Birch & Jacobs, 1979), more than 20 times worse than optimum acuity in man. It is commonly assumed that the large size of the receptive field and the poor acuity reflect neural processing and not optical spread. Part of the reason for thinking this is that an acuity of 0.05 min^{-1} is so far from limits set by diffraction, even with small pupils, that it is difficult to imagine that this acuity is not simply a reflection of the coarse neural grain with which information is processed by the rat visual system. Consistent with this, if one assumes that the rat retina is much like the human peripheral retina and takes into account the differences in eye size, the 8 cycle/deg resolution limit at 12 deg in the human peripheral retina (Daitch & Green, 1969) corresponds to 1.3 cycles/deg in the rat and 0.6 cycle/deg in the mouse, values which are very close to the limits of what rats and mice can actually see (Birch & Jacobs, 1979; Sinex et al., 1979). Thus, one is inclined to think that the rat and mouse retina is much like the human peripheral retina. It is important to note in this regard that direct measurements in man show that the low acuity in the near periphery is mainly due to the neural processing and not to optical degradation of the peripheral image (Green, 1970; Artal et al., 1995*a*; Williams et al., 1996). Supportive evidence for optics being of relatively minor importance in limiting rat vision comes from Brown (1965) who reported that the size of the experimentally determined ganglion cell receptive-field centers was comparable to the size of the anatomically determined dendritic tree of the ganglion cells. The receptive-field data was obtained using small spots of light which were projected onto a screen in front of the animal (Brown & Rojas,

Correspondence and reprint requests to: Daniel G. Green, Neuroscience Building, 1103 E. Huron Street, University of Michigan, Ann Arbor, MI 48104-1687, USA.

1965). If optical spread were significantly enlarging the retinal images of spots, then the measured receptive fields should have been larger than the true physiological receptive fields.

However, the situation might not be quite so simple. When one views the rat fundus with an ophthalmoscope, the images of the retinal landmarks, such as fine blood vessels, do not appear to be as sharp and clearly delineated as in man. Hughes and Wassle (1979) have quantified these observations by using indirect ophthalmoscopy to view the retinal images of square-wave grating targets. They reported that the double-pass retinal image was so poor that at about 3 cycles/deg the contrast of the retinal image dropped to zero. Given recent advances in the technology for making objective measurements of retinal image quality using the double-pass apparatus (Santamaría et al., 1987; Artal & Navarro, 1992; Artal et al., 1995*b*, Williams et al., 1996), we decided it was appropriate to make detailed measurements of the double-pass line spread in rats and mice. Such measurements had been made on the cat eye (Bonds et al., 1972; Bonds, 1974), but not on rodent eyes. One motivation for knowing what sets the limits to spatial resolution in rodent eyes is that small rodents have become increasingly more important as experimental animals as new developments in genetics have created the potential for good rodent models of hereditary human eye disease.

We report here that even with a 1-mm pupil, rat and mouse retinal image quality is very poor relative to the limits imposed by diffraction. With a 1-mm pupil, the image of a thin line spreads not over several minutes of arc, as in man, but rather over as much as several degrees of visual angle. It was surprising therefore to discover that in spite of the low quality of the image that is formed on the retina, the optics of the eye does not set the limits for spatial vision. In fact, the optics and the retinal properties seem to be sufficiently well matched that better optics would lead to only very slight improvements in the visual capacities of both rats and mice. Thus, the situation is much like that in the fovea of man (Campbell & Green, 1965), but on quite a different spatial scale.

Methods

Double-pass technique

An improved double-pass apparatus was developed to measure the modulation transfer function in the human eye. The description of this system along with the MTF results under different conditions have been presented elsewhere (Santamaría et al., 1987; Artal & Navarro, 1992, 1994; Navarro et al., 1993; Artal et al., 1995*b*, Williams et al., 1996). The system we used in this work consists of two stages: the recording of short-exposure coherent aerial images of a point object after double pass through the eye; and digital image processing, including averaging of aerial images, Fourier transform, and computation of the square root to obtain the "single pass" ocular MTF.

We have modified the double-pass apparatus for use in rodent's eyes. Fig. 1 shows a diagram of the experimental setup. The beam coming from a red He–Ne laser ($\lambda = 632.8$ nm) of nominal power (10 mW) first passes through an optional neutral density filter (DF) used to attenuate and adjust the light intensity on the CCD camera to the optimum range. The beam is spatially filtered by a 20× microscope objective (M). A 10-μm pinhole (P) acts as the point object (O). The emerging beam is collimated by the lens LC ($f' = 200$ mm); about 8% of the light is reflected towards the eye by a pellicle beam splitter (BS). Before entering the eye, the beam passes through a system consisting of two equal lenses L1–L2

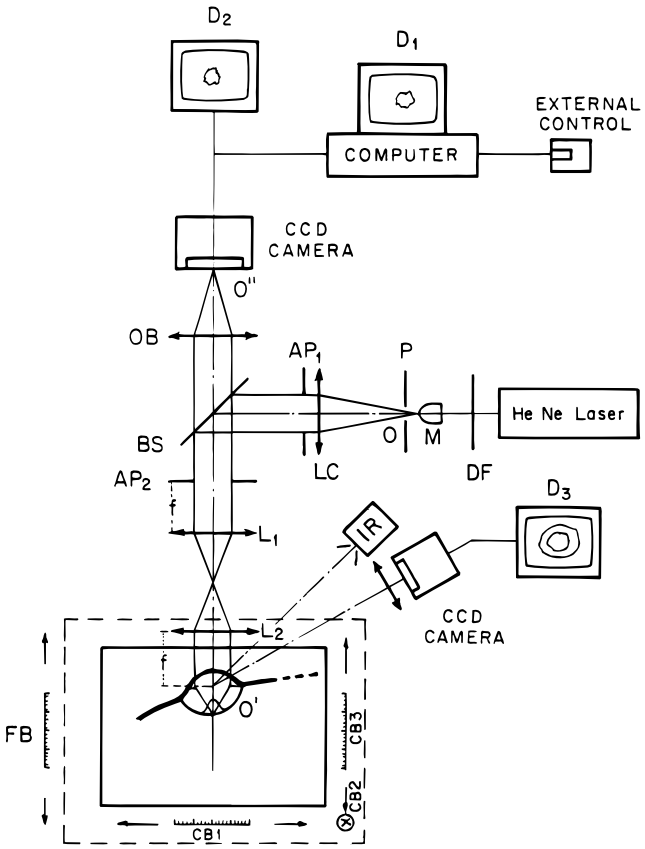

Fig. 1. Diagram of the experimental setup.

($f' = 120$ mm). This allows use of an artificial pupil by imaging the spot (AP2) on the animal's pupil plane by the lenses L1–L2, independent of their relative position. This provides a method to modify the state of focus by moving backward and forward the block (FB), to which the animal in the stereotaxic apparatus is fixed. The animal's eye is centered with respect to the measurement beam by using two translation stages (CB1, CB2) and the eye is placed at one focal length distance from lenses L2 by using a third translation stage (CB3). The animal's eye forms the image of the point O on the retina O′, and a small fraction of the light is reflected back, passing again through the optical media of the eye (second pass), lenses L1–L2, and the beam splitter (BS). Finally, an objective lens (OB) ($f' = 28$ mm) forms the aerial image O″ on a CCD camera. The camera (Hitachi KP-140) along with the frame grabber (Matrox MVP-AT) was previously calibrated. Each pixel subtends 1.28 min of arc, with the whole 256 × 256 pixel images covering nearly 5.5 deg of visual field. The double-pass retinal image of the point test was monitored in real time (D2) allowing us to control centering and other factors prior to digitizing and storing the images using the frame grabber. The measurements were obtained for different focus positions from −10 diopters to 15 diopters, adjusted by placing the block (FB) in different positions. The short-exposure aerial images were averaged to remove speckle noise to simulate incoherent imaging conditions (Santamaría et al., 1987). In this particular study, we computed each MTF from the average of 16 frames. The actual procedure is to take two series of eight exposures each and compute the average afterwards. Each snapshot is delivered by the experimenter when the desired conditions are reached. The centering of the animal's eye is checked

before taking each image, and the resulting image is accepted only when it is free of artifacts and the intensity is within a useful range. A background image is obtained by placing a black diffuser in the pupil plane instead of the eye and subtracted from the primary image. After averaging the short-exposure retinal images, the remaining background is removed by subtracting the average intensity value computed in the four corners of the image. The Fourier transform of the aerial image is computed, and the "single pass" MTF is obtained as the square root of its modulus.

Animal manipulation

Six hooded Long Evans rats (four males and two females) 3 months of age were used in these experiments and three male pigmented (C57BL/6J) mice of about the same age. The animals were anesthetized with i.p. injections of Equistesin (3 ml/gm). Supplementary doses were administered every 30 min. Body temperature was maintained by placing the animal on a heating pad. All the measurements were from the animal's right eye. The animal's eyelids were retracted with surgical silk thread. Animals were mounted on a Kopf small-animal stereotaxic apparatus (model 900) that allowed for an unobstructed view of the right eye. A suture placed through the conjunctiva allowed us to rotate the eyeball so as to bring the axis of the eye into approximate alignment with the axis of the measuring system. As Hughes (1977) had previously reported, we found that it was essential to keep the cornea moist. Artificial tears were applied on a regular basis throughout the experiments. Just before the collection of each set of data, a drop was placed on the eye and the excess removed with a small piece of absorbent tissue. An ancillary infrared viewing system allowed us to monitor and measure the size of the animal's pupils. After the animal had been aligned, initial measurements could be made through the natural pupil. In the anesthetized animal in a well-illuminated room, the pupil typically varied from about 1 to 2 mm in diameter. Following these initial measurements the pupil was dilated with atropine (1%). It took about 10 min for the pupil to reach a fully dilated diameter of 3.5 and 4 mm. Additional measurements were then obtained through an artificial pupil projected into the dilated natural pupil.

Results

Focus

In the first set of experiments, we attempted to determine the plane of best focus in the rat's eye. While the whole question of the refractive state of the rat's eye has been a matter of some controversy (see Hughes, 1977 for a review), our interest was simply in determining what focus gave us the sharpest images. The approach we took was to record double-pass images in each eye. Using the double-pass line spread function, we determined how the width of the double-pass image changed with varying focus. The vergence of the incoming pencil of rays was varied by changing the position of lens L_2 and animal relative to lens L_1 (Fig. 1). Sample double-pass aerial images from one animal are shown in Fig. 2. These aerial images were formed on the CCD camera with pupil diameters of 1 and 2 mm and ± 12 diopter extremes in the vergence of the incoming bundle. The images on the left, labelled hyperopic, are for a converging incoming bundle of rays ($+8.4$ diopters) and those on the right are for a diverging bundle (-8.4 diopters). These images are more or less radially symmetrical, as were all the double-pass images we obtained. For both pupil sizes illustrated,

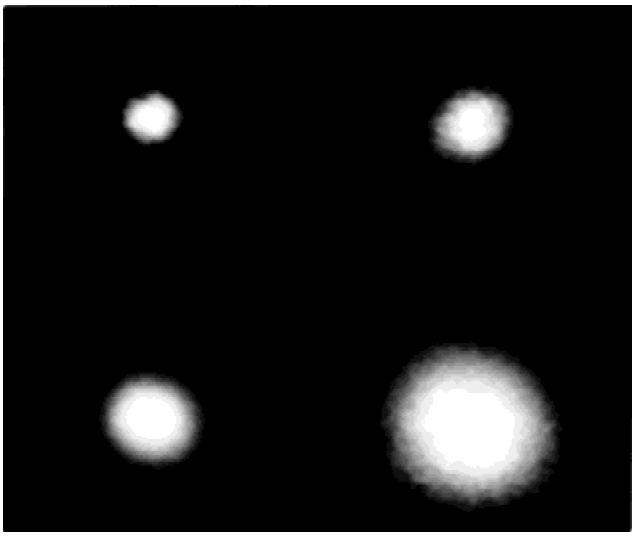

Fig. 2. Two-dimensional double-pass images of a rat's eye for two pupil diameters and two refractions (8.4 diopters on the left and -8.4 diopters on the right). The upper images are for a 1-mm pupil and the lower images for a 2-mm pupil.

the double-pass images were narrowest when the eye was hyperopic. Fig. 3 shows one-dimensional double-pass line functions for the aerial images shown in Fig. 2. They were obtained from the two-dimensional point spread function by integrating the measurements vertically. As Figs. 2 and 3 demonstrate, the images were sharper when the eye was hyperopic. The question which remains unanswered is where exactly was the eye focused? To establish this, measurements of the retinal image were made in which focus was systematically varied over a range of -8.4 to 12.6 diopters. From each of the double aerial point spread functions, a horizontal double-pass line spread function was computed. Using these line spread functions, we determined the width of the double-pass image at half-height. The results of such measurements with two pupil sizes in three pigmented rats are shown in Fig. 4. Panel A, on the left, is for a 1-mm pupil, and panel B, on the right, is for a 2-mm pupil. With a 1-mm pupil, the width of the double-pass functions are quite flat, particularly on the positive (hyperopic) side of emmetropia. For the vergence of the incoming rays varying between 0 and $+8.4$ diopters, the width of the double-pass spread function did not vary by more than 10%. In other words, over this whole range the changes are so small that the image is really in equivalent focus. In this regard, it is important to note that we have plotted the width of the double-pass point spread function. The actual changes in the quality of the image on the retina, the single-pass spread function, would be expected to be still smaller (see Fig. 8 for a comparison of single- and double-pass point spread functions). This great depth of focus is consistent with ± 10 diopters predicted by Green et al. (1980). Nonetheless, there was a clear tendency for the image to be sharper at 8.4 than at 0 diopters.

With 2-mm-diameter pupils, the image quality was considerably worse. The double-pass spread functions were about a factor of two broader than with the 1-mm pupil. In addition, the tendency for the images to be sharper when the bundle of incoming rays was hyperopic was much clearer. There were also larger differences between animals with the 2-mm pupils than with the 1-mm pupils. These differences could be due to differences in the refractive state

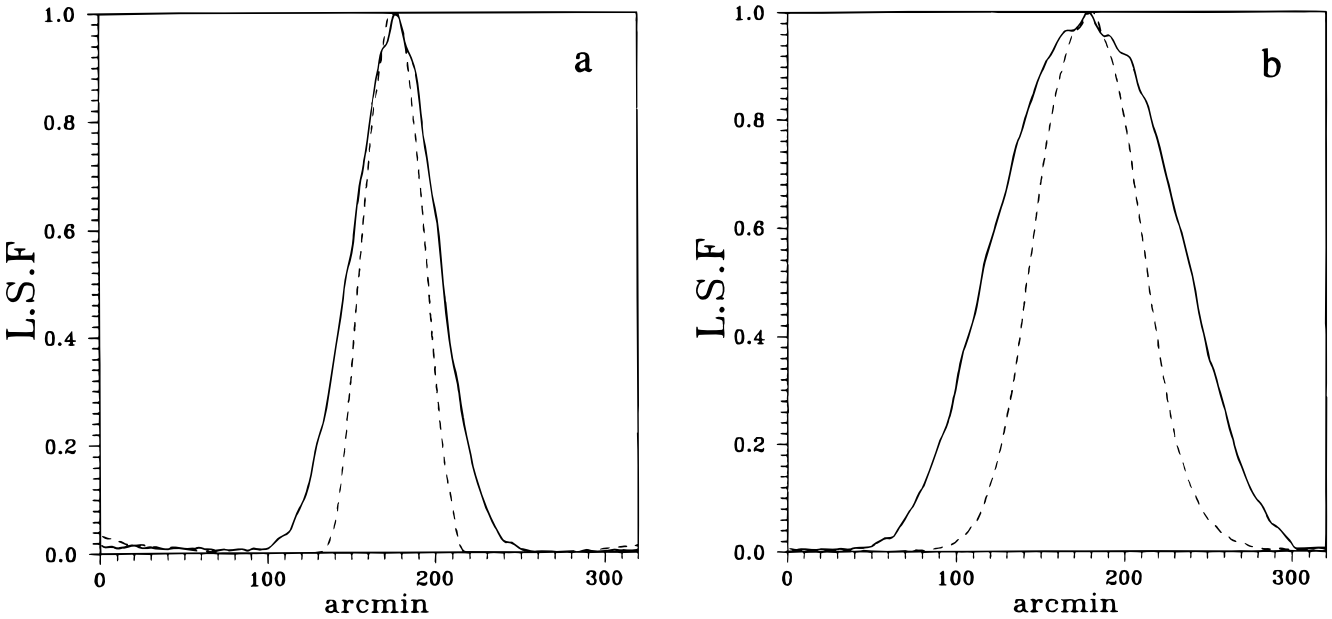

Fig. 3. One-dimensional double-pass line spread functions. (a) 1-mm pupil diameter (−8.4 diopters—solid line and 8.4 diopters—dashes), and (b) 2-mm pupil diameter (from double-pass images illustrated in Fig. 2).

with the larger pupils. The animal shown with squares was 5 diopters more hyperoptic (and the animal shown with circles was 10 diopters more hyperopic) than the animal shown with the triangles.

Fig. 5 shows some results for a mouse. A typical double-pass line spread function is plotted in Fig. 5a. If one compares this with the line spread functions of Fig. 3, it is clear that the width of the double-pass spread function in the mouse is nearly three times as broad as that in the rat. Fig. 5b shows that, in addition to the overall image quality being worse in the mouse, there seems to be less of a tendency for the width of the spread function to change with refraction, as would be expected for a smaller eye (Green et al, 1980).

Accommodation

It is generally believed that the rat cannot accommodate. Rats are reported to lack the ciliate muscles required to change the curvature of the ocular lens. Also one might argue that since the rat eye is already so hyperemic, any change in refractive power would do little to bring near targets into better focus. Nonetheless, we decided to take advantage of the opportunity we had of testing for accommodative ability by comparing the changes in the double-pass image size with focus with "unparalyzed" accommodation and with accommodation "paralyzed" with atropine. Fig. 6 shows a comparison of the width of the recorded double-pass images as

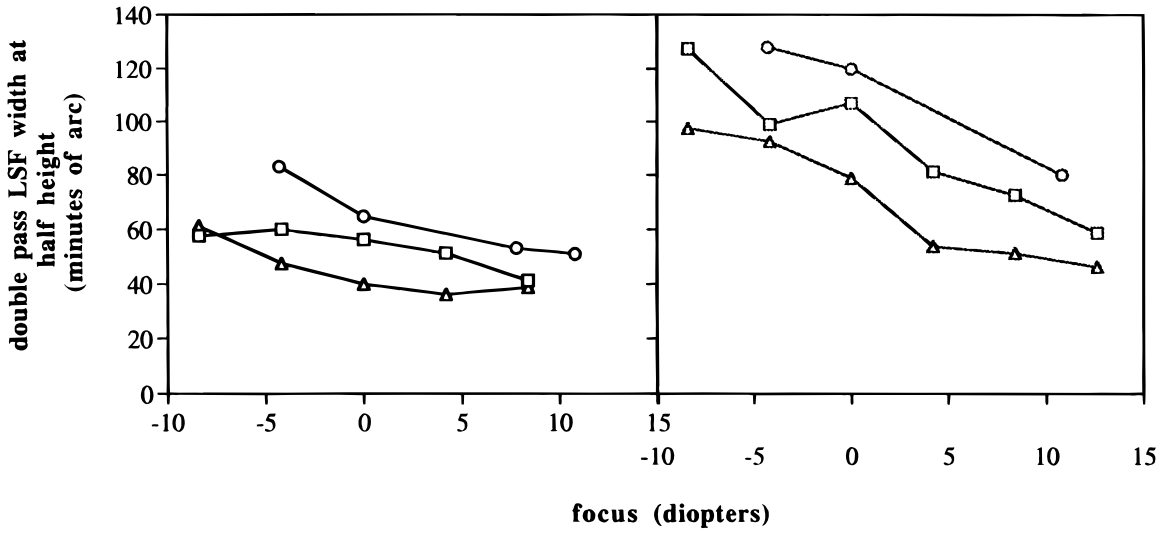

Fig. 4. Width at half-height in the double-pass images for three animals for two pupil diameters (1-mm pupil in left panel and 2-mm pupil in right panel).

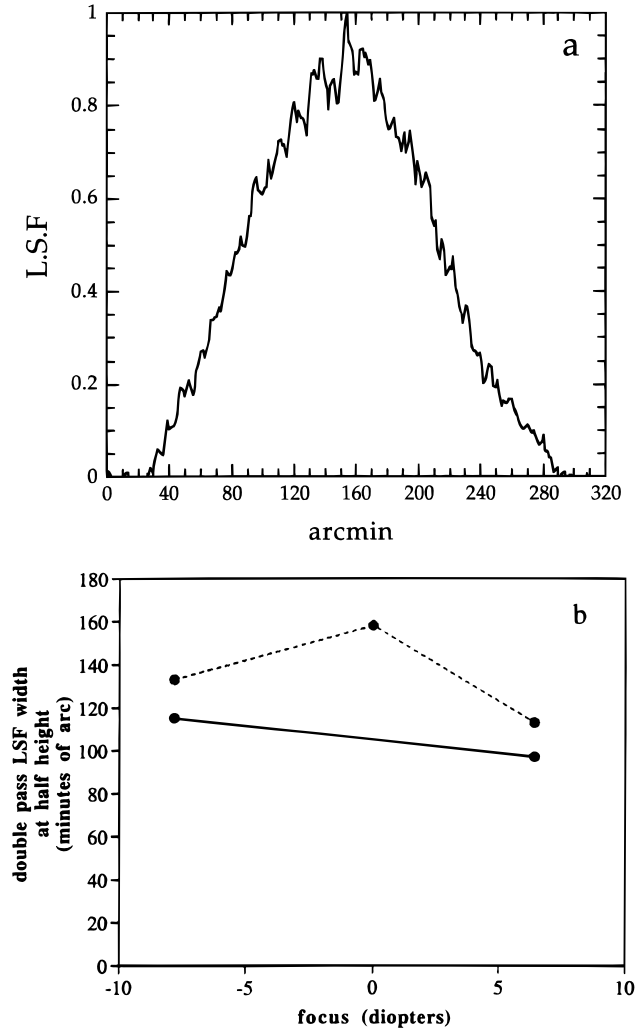

Fig. 5. (a) One-dimensional double-pass line spread functions for 1-mm pupil diameter and best focus in a mouse. (b) Width at half-height in the double-pass retinal images of a mouse for two pupil diameters, with artificial pupils, and atropine.

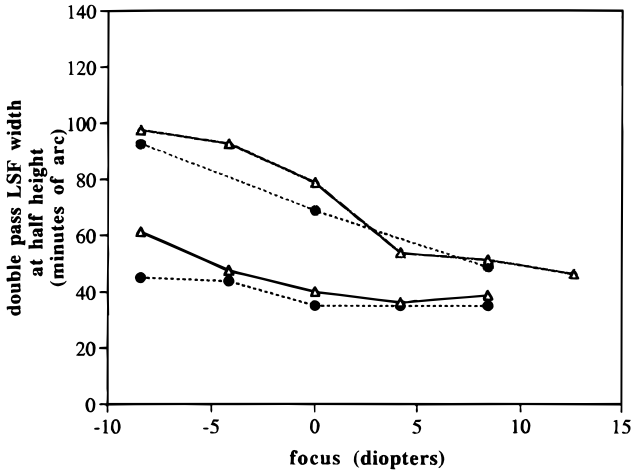

Fig. 6. Width at half-height of the double-pass line spread functions as a function of focus for one rat with atropine (solid line) and without atropine (dashed line), for two pupil diameters (1 and 2 mm).

a function of focus in the same animal with and without atropine, for 1- and 2-mm pupil diameters. We found no significant changes with atropine. The width of the double-pass line spread function consistently was slightly smaller with the natural pupil. This could be due to the natural pupil actually being a little smaller than the artificial pupil or to the natural pupil being better centered than the artificial pupil. The absence of any indication of a change in refractive power with atropine is consistent with the rat lacking the ability to accommodate. These experiments, of course, showing that atropine produces no additional change in refractive power, do not prove that the rat does not have the ability to accommodate, since under these conditions of anesthesia accommodation could already be fully relaxed.

Single-pass optical quality

What is the quality of the retinal image in the rat (and mouse)? To do this, we have taken the double-pass aerial images and used them to calculate modulation transfer functions. Fig. 7 shows the average modulation transfer functions with 1- and 2-mm pupils, on linear scales (a) and on a logarithmic modulation scale (b). From these MTFs, it is relatively straightforward to calculate the (single-pass) point spread of the eye. Fig. 8 shows the average point spread function obtained in four rats for the conditions of best focus (8.4 diopters hyperopic) with a pupil size of 1 mm. The single-pass point spread function has two components, a relatively narrow peak (about 3 minutes of arc half-width) and a broad pedestal. Fig. 9 shows the MTFs for one rat at the extremes of hyperopic and myopic. The optical quality in the rodents' eyes in comparison with those in the human eye is exceedingly poor.

The MTF with the 1-mm pupil fell to less than 0.1 at about 2.0 cycles/deg. Fig. 10 further illustrates the differences between rodents and man by comparing human and rat and mouse MTFs. The MTF of the mouse has a high frequency cutoff of only 1.0 cycle/deg. Since the rat's eye is about one fifth the size of the human eye, we have compared the MTFs measured with the 4-mm pupil with the measurements at 1 mm, so that the numerical apertures are approximately equivalent. Fig. 10 also shows measurements that were obtained in the mouse eye with a 1-mm pupil.

MTF calculations from a rat's model eye: Comparison with the measured MTFs

It is of interest to know how our measurements compare with what might be expected. To address this, we have used a simple model of the rat's eye to calculate the retinal MTF. We performed the calculations by using the ZEMAX XE optical design software (Focus Software, Tucson, AZ). The rat's eye was modeled by a series of spherical refracting surfaces. The curvatures and positions of the refracting surfaces of the rat's eye were taken from Block (1969). Figs. 11a and 11b show a comparison of calculated and measured MTFs for 1- and 2-mm pupils. The model correctly predicts that image quality is much worse than the diffraction limit, with a 2-mm pupil. The calculated and measured MTFs agree reasonably well below 1 cycles/deg, but the measurements systematically fall below the calculations at higher spatial frequencies. This may be due to the point spread function being a sum of a narrow function, which is accounted for by the model, and a

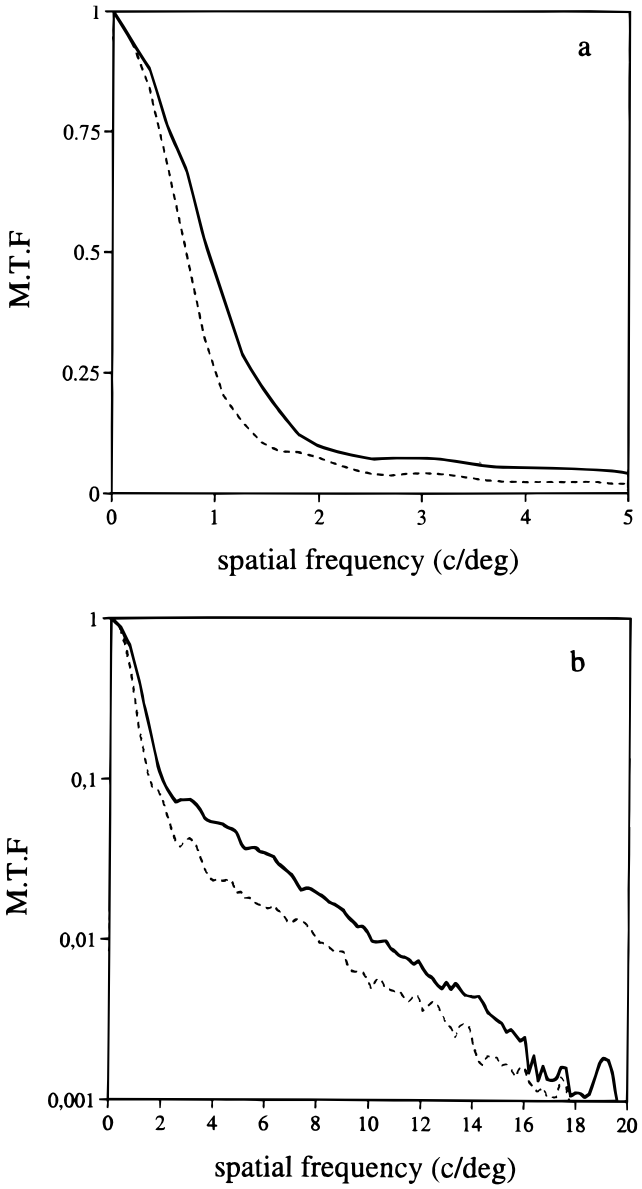

Fig. 7. Average modulation transfer functions with 1-mm (solid line) and 2-mm pupils (dashed line) in best focus (8.4 diopters hyperopic). (a) On a linear modulation scale. (b) Same data over an expanded spatial-frequency range on a logarithmic modulation scale. The curves are the averages from four rats.

broad function which adds a wide pedestal (see Fig. 8), which is not accounted for by the model. Thus, the loss in image quality is not completely explained by simple spherical aberration. In the small eye of the rat, 2 mm corresponds to 6 mm in man. In the human eye with a 6-mm pupil, higher order aberrations cause significant deviations from the diffraction limit (Campbell & Green, 1965). Fig. 11c shows that the model eye exhibits great depth of focus. The calculated image modulation at 2 cycles/deg changes very little when focus varies from −8 to 16 diopters.

Discussion

We began by determining the refractive state of the rat. To find the refraction that produced the sharpest retinal images, we varied the

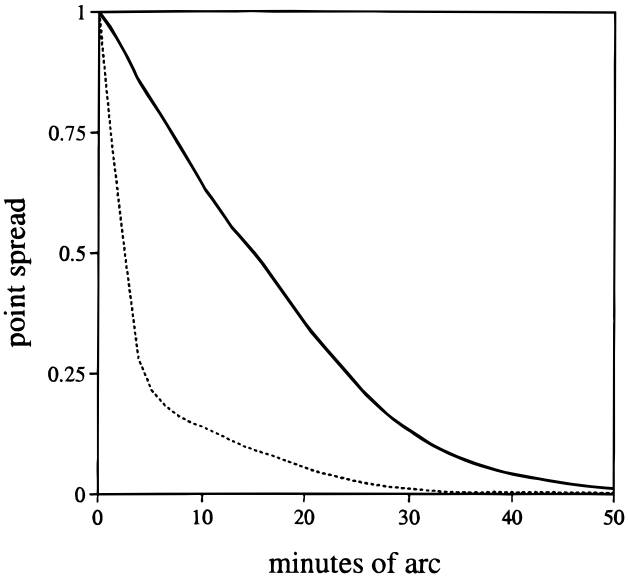

Fig. 8. Average double- (solid line) and single-pass (dashed line) point spread functions for rats.

vergence of the source over a range of 21 diopters (−8.4 to 12.6 diopters). This corresponds to object distances from 12 cm in front of the eye to way beyond optical infinity. We found only a very weak dependence of image quality on focus, with a tendency for the spread function to get slightly narrower when the eye was extremely hyperopic. Thus rodent eyes have great depth of focus. We did not make measurements under still more hyperopic conditions. While it seems possible that the image might be a little bit sharper with greater hyperopia, any such improvement in image quality would have to be very small. Such improvement, if it occurred, would be of no physiological relevance to an animal that must view things in the space between its eyes and optical infinity.

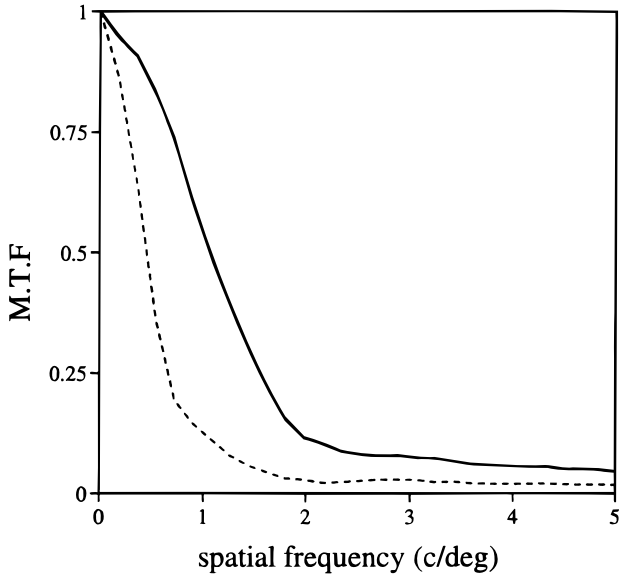

Fig. 9. MTFs for a single animal with extremes of hyperopia and myopia (−8.4 diopters—dashed line and 8.4 diopters—solid line, respectively).

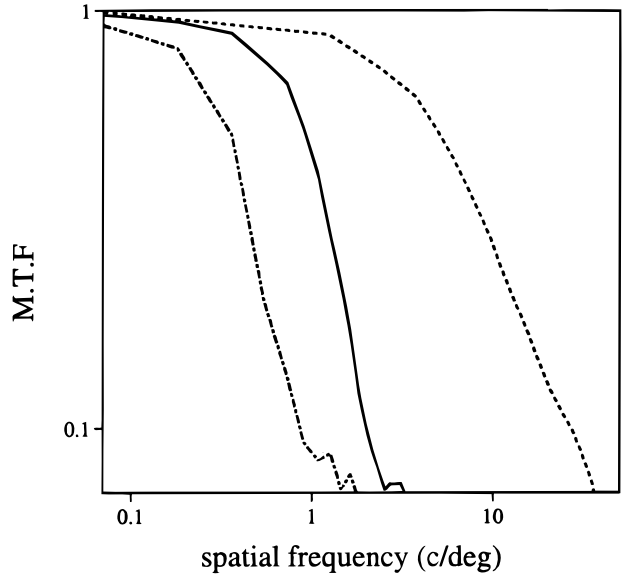

Fig. 10. MTFs on logarithmic scales of a rat (solid line), a mouse (dot-dashed line), and a typical human observer (dashed line).

Hyperopia has been found previously by those using other retinoscopic techniques. It has been suggested that the hyperopia seen in small eyes arises because the light that returns comes from the vitreal-retinal surface which is 100–150 μm in front the photoreceptors (Glickstein & Millodot, 1970). There is nothing in this study for or against this idea. We accept that this, in addition to the fact the measuring light is a 632.7-nm laser, may explain the 10–15 diopters of hyperopia. It is said that rats and mice lack the ability to accommodate. When we examined the effect that atropine had on the state of focus, we saw no changes. This is consistent with, but does not prove, inability to accommodate.

The detailed measurements of the optical quality of the retinal images in the rat and the mouse are new and potentially interesting findings. Moreover, it was surprising to discover that in comparison to images in other animals the quality of the retinal image in rodents was very poor. In man with a 1-mm pupil, the retinal image is essentially diffraction limited, i.e. the cutoff frequency is 30 cycles/deg. In rat, the cutoff is closer to 1.5 or 2.0 cycles/deg. In mice, the quality was still worse with the optical limit being close to 1.0 cycle/deg. One of the limitations of the double-pass technique is that it does not measure the broad veiling pedestal of light that the direct measurements of Robson and Enroth-Cugell (1978) showed to exist in the cat's eye. This is particularly true in these experiments where a background image, obtained by placing a black diffuser in the pupil plane instead of the eye, was subtracted from the primary image and the remaining background was removed by subtracting the average intensity value computed in the four corners of the image. Thus, the broad veiling pedestal that must surely exist in the rodent's eye has not been measured. Thus, the MTFs we present here almost certainly overestimate the true contrast at each spatial frequency by some small but unknown factor.

Are these poor images the cause of the poor spatial resolving abilities of mice and rats? The fall in optical performance with increasing spatial frequency is always due to a combination of optical and neural factors. The question is, in the rat, how much of this fall is contributed by optics as opposed to neural processing? To address this issue one needs to compare the optics with the

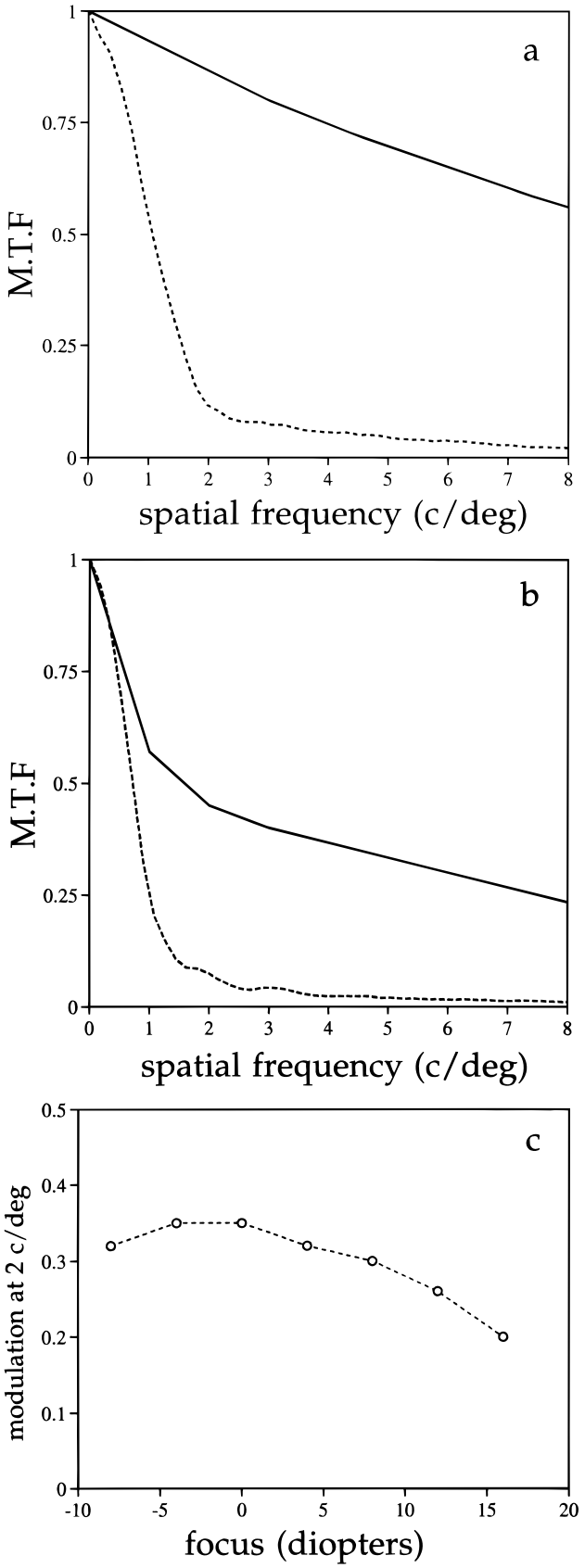

Fig. 11. Calculated (solid line) and measured MTFs (dashed line). (a) For a rat in best focus with 1-mm pupil. (b) For a rat in best focus with 2-mm pupils. (c) The calculated change in modulation at 2 cycles/deg produced by various amounts of defocus. The calculations are for the rat's eye with a 1-mm pupil.

overall contrast sensitivity function. Birch and Jacobs have measured the contrast sensitivity function (CSF) of rats using behavioral methods and their measurements are well fitted by the function

$$CSF = k_1 \exp(-k_2 f), \quad (1)$$

where k_1 is a constant that depends on the average intensity, $k_2 = 2.88$ deg/cycle, and f is spatial frequency in cycles/deg. Fig. 12a compares our measured MTF with their CSF. Both are drawn on a linear spatial-frequency axis. The modulation of the optical image is plotted on the left vertical axis and contrast sensitivity is plotted on the right axis. Surprisingly, even though the retinal image is of poor quality, the optical MTF falls more slowly with increasing spatial frequency than the CSF. These measurements suggest that optics is not the major factor limiting visual resolution. At 1 cycle/deg, close to the limit of resolution, the behavioral contrast sensitivity function of Birch and Jacobs has fallen by a factor 20. Our measurements of the optical MTF(circles in Fig. 12a) show that at 1 cycle/deg the optics causes about a factor of 2 reduction in contrast on the retina. Thus, the majority of the reduction, the remaining factor of 10, must be due to the neural processing.

Another way of looking at the effect of the optics is to use the measured optical MTF to calculate what the CSF would be if the optics were perfect. This result is also shown in Fig. 12 (the triangles). When one compares the CTF the eye could achieve with perfect optics (triangles), against the actual CTF (squares), it is apparent that better optics would lead to only small improvements in acuity. Perfect optics would increase resolution by only one Snellian line. Thus, the optics and visual capacities are matched in the sense that the optics are not much better than they need be to cause vision to be primarily limited by neural factors.

The situation is reminiscent of the human fovea where Campbell and Green (1965) found that at higher spatial frequencies the attenuation due to the nervous system was twice as great as that due to the optics. This kind of arrangement makes good sense from an evolutionary perspective. If the reverse were true, that is if better optics would lead to better vision, then evolutionary pressure would be expected to select those animals with better optics. On the other hand, there is nothing to be gained by having fine spatial detail present in the retinal image if the neural apparatus cannot process this information. In this context, the poorer optical quality in the mouse is consistent with its lower spatial resolving capacities. This matching of the optical quality to the spatial abilities of retina–brain seems to be a general finding. In cat, frog, rat, and mouse (Wassle, 1971; Bonds, 1974; Robson & Enroth-Cugell, 1978; Krueger & Moser, 1971; and present study), where the visual capabilities are less than those of man, the optical quality of the retinal image is progressively worse. On the other hand, in the eagle, which has foveal resolving capacities greater than in the human fovea, the optical quality is higher than in the human fovea (Shlaer, 1972). In this context, we may tend to take for granted the ability of living creatures to specialize and refine cellular structures so that they are sufficiently clear, smooth, and regular to form good optical images on their retinas. It would seem that there is a cost associated with doing this and the cost is sufficiently great that each organism does no better in refining the optical quality of its dioptric apparatus than necessary.

One aspect of this work puzzled us. What is causing the images in the rat to be so poor? Could it simply be the small eye itself? To address this issue, we traced rays through an optical model of the rat's eye consisting of a series of smooth spherical surfaces with curvatures and indices that come from the rat schematic eye of Block (1969), Campbell and Hughes (1981), and Hughes (1979). For a 1-mm pupil, these calculations give the MTFs plotted in Fig. 11. While the agreement is not perfect, it is better than we expected, particularly since no aberrations other than simple spherical aberration have been included in the model. Thus, it seems that in a small eye simply having strongly curved spherical refracting surfaces can be sufficient to cause poor retinal images, and thus one might not expect small eyes to have high acuity. This is not the complete story of why rodent optical images are poor. In addition to having highly curved spherical refracting surfaces, rat and mouse eyes must have higher order aberrations that cause image quality to be worse than what we calculate from our model eye.

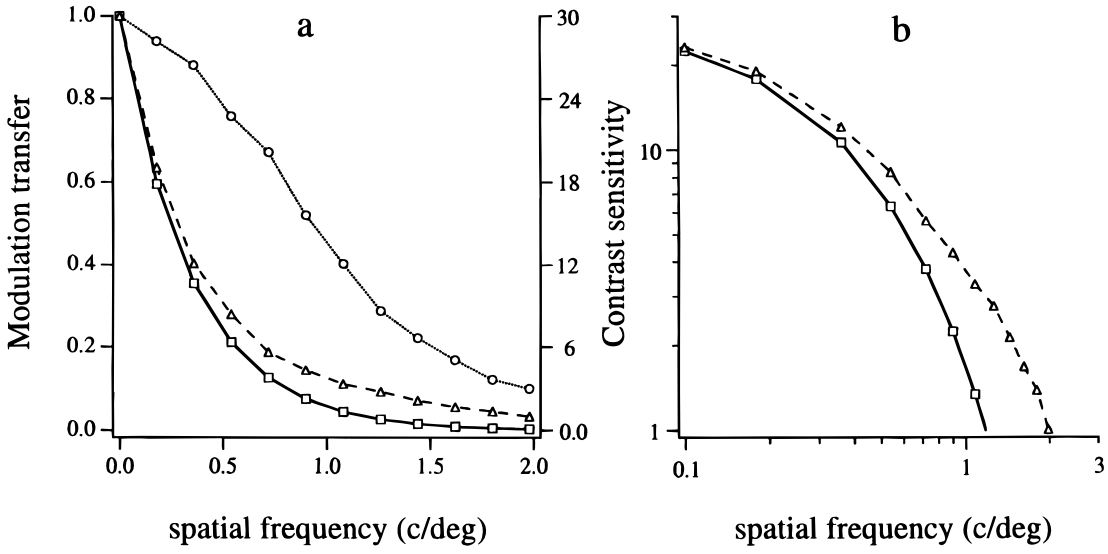

Fig. 12. Effect of optics on rat contrast sensitivity. (a) The average modulation transfer function of the rat (from Fig. 8) is plotted with circles. The normalized behavioral contrast sensitivity of the pigmented rat (after Birch & Jacob, 1979) is plotted with squares. The computed retinal contrast is plotted with triangles. (b) A comparison of the actual contrast sensitivity of the hooded rat (squares) with what would be expected if the optics were perfect (triangles).

Acknowledgments

This research was supported by a NATO collaborative research grant to P. Artal and D.G. Green (CRG 940081); a grant from DGICYT, Spain, to P. Artal (PB94-M38-CO2-01); and a grant from the National Institutes of Health, US Public Health Service to D.G. Green (EY 00379).

References

Artal, P. & Navarro, R. (1992). Simultaneous measurement of two-point-spread functions at different locations across the human fovea. *Applied Optics* **31**, 3646–3656.

Artal, P. & Navarro, R. (1994). Monochromatic modulation transfer function of the human eye for different pupil diameters: An analytical expression. *Journal of the Optical Society of America A* **11**, 246–249.

Artal, P., Derrington, A.M. & Colombo, E. (1995*a*). Refraction, aliasing and the absence of motion reversals in peripheral vision. *Vision Research* **35**, 939–947.

Artal, P., Iglesias, I. López-Gil, N. & Green, D.G. (1995*b*). Double-pass measurements of the retinal image quality with unequal entrance and exit pupil sizes and the reversibility of the eye's optical system. *Journal of the Optical Society of America A* **12**, 2358–2366.

Balkema, G.W. & Pinto, L.H. (1982). Electrophysiology of retinal ganglion cells in the mouse: A study of a normally pigmented mouse and a congenic hypopigmentation mutant pearl. *Journal of Neurophysiology* **48**, 968–980.

Birch, D. & Jacobs, G.H. (1979). Spatial contrast sensitivity in albino and pigmented rats. *Vision Research* **19**, 933–937.

Block, M.T. (1969). A note on refraction and image formation in the rat's eye. *Vision Research* **9**, 705–711.

Bonds, A.B. (1974). Optical quality of the living cat eye. *Journal of Physiology* (London) **243**, 777–795.

Bonds, A.B., Enroth-Cugell, C. & Pinto, L.H. (1972). Image quality of the cat eye measured during retinal ganglion cell experiments. *Journal of Physiology* (London) **220**, 383–401.

Brown, J.E. (1965). Dendritic fields of retinal ganglion cells of the rat. *Journal of Neurophysiology* **28**, 1091–1100.

Brown, J.E. & Rojas, J.A. (1965). Rat retinal ganglion cells: Receptive field organization and maintained activity. *Journal of Neurophysiology* **28**, 1073–1090.

Campbell, F.W. & Green, D.G. (1965). Optical and retinal factors affecting visual resolution. *Journal of Physiology* (London) **181**, 576–593.

Campbell, M.C. & Hughes, A. (1981). An analytic, gradient index schematic lens and eye for the rat which predicts aberrations for finite pupils. *Vision Research* **21**, 1129–1148.

Daitch, J.M. & Green, D.G. (1969). Contrast sensitivity of the human peripheral retina. *Vision Research* **9**, 947–952.

Friedman, L.J. & Green, D.G. (1982). Ganglion cell acuity in hooded rats. *Vision Research* **22**, 441–444.

Glickstein, M. & Millodot, M. (1970). Retinoscopy and eye size. *Science* **163**, 605–606.

Green, D.G. (1970). Regional variations in the visual acuity for interference fringes on the retina. *Journal of Physiology* (London) **207**, 351–356.

Green, D.G., Tong, L. & Cicerone, C.M. (1977). Lateral spread of light adaptation in the rat retina. *Vision Research* **17**, 479–486.

Green, D.G., Powers, M.K. & Banks, M.S. (1980). Depth of focus, eye size and visual acuity. *Vision Research* **20**, 827–835.

Hughes, A. (1977). The refractive state of the rat eye. *Vision Research* **17**, 927–939.

Hughes, A. (1979). A schematic eye for the rat. *Vision Research* **19**, 569–588.

Hughes, A. & Wassle, H. (1979). An estimate of image quality in the rat eye. *Investigative Ophthalmology and Visual Science* **18**, 878–881.

Krueger, H. & Moser, E.A. (1971). Refraktion und Abbildungsgüte des Froschauges. *Pflügers Archiv* **326**, 334–340.

Lashley, K.S. (1938). The mechanisms of vision III: The comparative visual acuity of pigmented and albino rats. *Journal of General Psychology* **37**, 481–484.

Muñoz Tedó, C., Herreros de Tejada, P. & Rodriguez Cañavate, A. (1992). Estudios fisiológicos y conductuales de la detección de frecuencias espaciales en roedores. *Investigaciones Psicológicas* **11**, 83–97.

Navarro, R., Artal, P. & Williams, D.R. (1993). Modulation transfer of the human eye as a function of retinal eccentricity. *Journal of the Optical Society of America A* **10**, 201–212.

Powers, M.K. & Green, D.G. (1978). Single retinal ganglion cell responses in the dark-reared rat: Grating acuity, contrast sensitivity, and defocusing. *Vision Research* **18**, 1533–1539.

Robson, J.G. & Enroth-Cugell, C. (1978). Light distribution in the cat's retinal image. *Vision Research* **18**, 159–173.

Santamaría, J., Artal, P. & Bescós, J. (1987). Determination of the point-spread function of the human eye using a hybrid optical-digital method. *Journal of the Optical Society of America A* **4**, 1109–1114.

Shlaer, R. (1972). An eagle's eye: Quality of the retina image. *Science* **176**, 920–922.

Sinex, D.G., Burdette, L.J. & Pearlman, A.L. (1979). A psychophysical investigation of spatial vision in the normal and reeler mutant mouse. *Vision Research* **19**, 853–857.

Stone, C. & Pinto, L.H. (1993). Response properties of ganglion cells in the isolated mouse retina. *Visual Neuroscience* **10**, 31–39.

Wassle, H. (1971). Optical quality of the cat eye. *Vision Research* **11**, 995–1006.

Wiesenfeld, Z. & Branchek, T. (1976). Refractive state and visual acuity in the hooded rat. *Vision Research* **16**, 823–827.

Williams, D.R., Artal, P., Navarro, R., McMahon, M.J. & Brainard, D.H. (1996). Off-axis optical quality and retinal sampling in the human eye. *Vision Research* **36**, 1103–1114.